The Journal of Comparative Neurology 517:616–632 (2009)
Research in Systems Neuroscience

Comparative, Three-Dimensional Anterior Sensory Reconstruction of *Aphelenchus avenae* (Nematoda: Tylenchomorpha)

ERIK J. RAGSDALE,[1]* PHUONG T. NGO,[1] JOHN CRUM,[2] MARK H. ELLISMAN,[2] AND JAMES G. BALDWIN[1]
[1]Department of Nematology, University of California, Riverside, California 92521
[2]National Center for Microscopy and Imaging Research, University of California, San Diego, La Jolla, California 92063

ABSTRACT

The anterior sensory anatomy (not including amphids) of the nematode *Aphelenchus avenae* (Tylenchomorpha) has been three-dimensionally reconstructed from serial, transmission electron microscopy thin sections. Models, showing detailed morphology and spatial relationships of cuticular sensilla and internal sensory receptors, are the first computerized reconstruction of sensory structures of a Tylenchomorpha nematode. Results are analyzed with respect to similarly detailed reconstructions of Rhabditida outgroup nematodes, *Acrobeles complexus* (Cephalobomorpha) and *Caenorhabditis elegans* (Rhabditomorpha). Homologies identified in *A. avenae* demonstrate the general conservation of the anterior sensory system between freeliving nematodes and the largely plant parasitic Tylenchomorpha. A higher degree of similarity is shown between *A. avenae* and *A. complexus*, with common features including: the presence of a second, internal outer labial dendrite (OL1); a second cephalic dendrite in the female (CEP2/CEM); an accessory process loop of inner labial dendrite 1; and terminus morphology and epidermal associations of internal sensory receptors BAG and URX. Unique to *A. avenae* is a pair of peripheral, lateral neurons of unknown homology but with axial positions and intercellular relationships nearly identical to the "posterior branches" of URX in *A. complexus*. Knowledge of homologies and connectivity of anterior sensory structures provides a basis for expansion of the experimental behavioral model of *C. elegans* to the economically important nematodes of Tylenchomorpha. J. Comp. Neurol. 517:616–632, 2009. © 2009 Wiley-Liss, Inc.

Indexing terms: *Acrobeles complexus*; *Caenorhabditis elegans*; Cephalobomorpha; fine structure; freeliving; homology; modeling; morphology; nematode; nervous system; plant parasitism; phylogeny; sensillum; transmission electron microscopy

Reconstruction of the nervous system in the model organism *Caenorhabditis elegans* (Ward et al., 1975; Ware et al., 1975; White et al., 1986; Hall and Russell, 1991) has been of immense utility in the study of its behavior. In particular, mapping of the anterior sensory system is critical for understanding responses coordinated though specific anterior receptors, which can have direct consequences for foraging and feeding (e.g., Kaplan and Horvitz, 1993; Hart et al., 1995; Sawin et al., 2000; de Bono et al., 2002). An impressive body of empirical knowledge has been amassed for this model system, but how far it can be applied to other nematodes is limited by our understanding of corresponding nervous structures across taxa. The case for comparative neurology is especially pressing in clades of parasitic nematodes, in which host searching and feeding behavior are the basis for species interactions of serious agricultural and economic concern.

Transmission electron microscopy (TEM) reconstruction of non-amphid sensory organs in the nematode *Acrobeles complexus* (Bumbarger et al., 2007) has demonstrated their high degree of conservation between distant, bacterial feeding taxa within the order Rhabditida. However, the extension of this model to plant parasitic nematodes within the order remains to be tested. A sister group relationship has been established between Cephalobomorpha (including *A. complexus*) and a clade of the largely plant- and insect-parasitic Tylenchomorpha (Aleshin et al., 1998; Blaxter et al., 1998; Holterman et al., 2006; Nadler et al., 2006; Smythe et al., 2006; Meldal et al., 2007; Bert et al., 2008). This phylogenetic frame-

Grant sponsor: US National Science Foundation; Grant numbers: TOL DEB 0228692 and PEET DEB 0731516; US Department of Agriculture; Grant number: 00903; US National Institutes of Health; Grant number: P41 PR04050.

*Correspondence to: Erik J. Ragsdale, Department of Nematology, University of California, Riverside, CA 92521.
E-mail: erik.ragsdale@email.ucr.edu

Received 12 March 2009; Revised 22 May 2009; Accepted 9 July 2009
DOI 10.1002/cne.22170
Published online July 17, 2009 in Wiley InterScience (www.interscience.wiley.com).

work suggests an opportunity for identifying homologies of anterior neurons and support cells in Tylenchomorpha with the aid of an intermediate, with which structures should be more readily recognizable.

To this end, we have conducted three-dimensional (3D) TEM reconstruction of the anterior sensory anatomy in the tylenchid nematode, *Aphelenchus avenae*. Explicit comparison is made to similarly detailed reconstructions from two outgroups, *A. complexus* in the immediate outgroup Cephalobomorpha and *C. elegans* in the more distantly related Rhabditomorpha. Because of its basal position within Tylenchomorpha, *A. avenae* is particularly well suited as a model for interpreting morphological transformations with respect to outgroups (Ragsdale et al., 2008). Understanding the primary neural interface between these nematodes and their environment necessarily has implications for host-parasite interactions. Moreover, comparative neurology between Tylenchomorpha and its immediate outgroup Cephalobomorpha is essential for addressing the evolution of parasitism.

The primary motivation for 3D TEM reconstruction of the sensory anatomy was to test extant molecular phylogenies by using morphological characters; this work has been conducted as part of a broader laboratory effort to establish a framework for studying the evolution of feeding morphology, particularly in plant parasites (Baldwin et al., 2004a,b; Bumbarger et al., 2006; Ragsdale et al., 2008). In spite of superficial morphological divergences between various Rhabditida, especially in the case of Tylenchomorpha, TEM data have revealed several aspects of mouthpart and anterior nervous morphology to be highly conserved (Bumbarger et al., 2006, 2007, 2009; Ragsdale et al., 2008), providing a potential avenue for discovery of characters informative at levels where they have been thus far lacking. Herein, results will be presented in a context of comparative systems neuroscience, with phylogenetic findings to be developed separately (Ragsdale, in preparation). The goal of the present work is to propose anterior sensory homologies necessary for extending the model of functional and behavioral neurology for *C. elegans* to Tylenchomorpha.

Nematode sensory structures include cuticular sensilla and internal receptors. Nematode cuticular sensilla fall into five classes, originally designated for *C. elegans* (White et al., 1986): inner labial sensilla (IL), quadrant outer labial sensilla (OLQ), lateral outer labial sensilla (OLL), cephalic sensilla (CEP), and amphids. Cuticular surface manifestations vary in form but are stereotypically arranged in concentric rings of six, the outer ring including cephalic sensilla and amphids, with some classes variously absent or not externally expressed in different nematode taxa. However, despite the considerable corpus of literature regarding sensory organs in Tylenchomorpha, including detailed line drawing reconstructions (Baldwin and Hirschmann, 1973, 1975; De Grisse, 1975, 1977; De Grisse et al., 1979; Endo, 1980; Trett and Perry, 1985), representation of some structures and subtle spatial interrelationships has not yet been implemented to the extent offered by 3D computer visualization.

Several types of internal receptors have been described in *C. elegans*. Homologous receptors have also been found in *A. complexus*, based on extensive positional similarity, but several differ considerably in their termini and presumably also in their function (Bumbarger et al., 2007). Preliminary evidence has shown similarities in the structure of putative homologs of at least some internal receptors between *A. complexus* and Tylenchomorpha, notably the BAG dendrite and to some extent URY (Bumbarger et al., 2007; Ragsdale et al., 2008). Although some internal receptors have been described for some species of Tylenchomorpha (Endo and Wergin, 1977; De Grisse et al., 1979; Trett and Perry, 1985), they are not yet sufficiently understood for adequate comparison with model outgroups. Furthermore, no detailed study of cuticular sense organs has been conducted on a nematode in Aphelenchoidea, a major and basal lineage within Tylenchomorpha (e.g., Holterman et al., 2006; Meldal et al., 2007). Recent advances in digital imaging and computer software for volume segmentation and model rendering offer a feasible approach to complete 3D reconstruction from serial TEM thin sections. Application of these tools to reconstruction of nematode sensilla has been demonstrated (Ashton et al., 1995) and since expanded to present a more detailed holistic picture of sensory apparati.

MATERIALS AND METHODS

Reconstructions presented herein are based on serial micrograph data used for those of the stylet and anterior epi-

Abbreviations

a	inner labial accessory neuron
aa	anterior arcade syncytium
ah	amphid sheath cell
am	amphid
ao	amphid socket cell
b	BAG sensory neuron
c	cephalic sensillum
c1	cephalic dendrite 1 (CEP1)
c2	cephalic dendrite 2 (CEP2)
ch	cephalic sheath cell
co	cephalic socket cell
f	FLP sensory neuron
fb	cephalic frame work blade
g	guiding apparatus
ha	HypA epidermal syncytium
hb	HypB epidermal syncytium
hc	HypC epidermal syncytium
hd	"HypD" epidermal cell
he	HypE epidermal syncytium
i	inner labial sensillum
i1	inner labial dendrite 1 (IL1)
i2	inner labial dendrite 2 (IL2)
ih	inner labial sheath cell
io	inner labial socket cell
o	outer labial sensillum
o1	outer labial dendrite 1 (OL1)
o2	outer labial dendrite 2 (OL2)
oh	outer labial sheath cell
oo	outer labial socket cell
pa	posterior arcade syncytium
pm	stylet protractor muscle
s	stylet/stoma
sm	somatic muscle
u	"unnamed lateral neuron"
x	URX sensory neuron
x′	URX lateral posterior process
y	URY sensory neuron

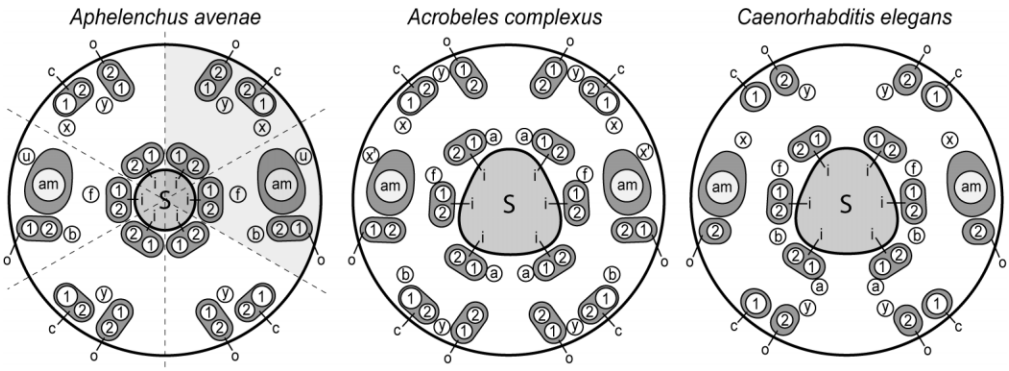

Figure 1.
En face drawing showing relative positions of cuticular sensilla and internal receptors in *A. avenae*, *A. complexus*, and the hermaphrodite of *C. elegans*. Broken lines separate six sectors, one lateral and one quadrant of which (shaded) have been fully reconstructed for *A. avenae* herein. The top of each diagram is dorsal. Numbers "1" and "2" refer to dendrites (IL1, OL1, CEP1 and IL2, OL2, CEP2, respectively) based on homologies assigned in the text. Letter codes for this and all subsequent figures are given in the abbreviations list. Information for *A. complexus* is redrawn from Bumbarger et al. (2007), and *C. elegans* from Ward et al. (1975).

dermis of *A. avenae* (Ragsdale et al., 2008) and thus include the same individuals and one additional specimen. Cultures of *A. avenae* (strain RGD103) were obtained courtesy of Dr. Robin Giblin-Davis (University of Florida-IFAS, Fort Lauderdale, FL) and maintained on *Monilinia fructicola* in LG potato dextrose agar medium. Adult, female nematodes were frozen in a Bal-Tec (Brookline, NH) HPM 010 high-pressure freezer and then dehydrated, fixed, and stained en bloc via freeze substitution by using a Reichert-Jung CS Auto freeze substitution apparatus (Reichert, Depew, NY) in an acetone cocktail of 3% osmium tetroxide and 1% uranyl acetate. Individuals were processed in custom stainless steel chambers to prevent specimen loss, as described by Bumbarger et al. (2006). Specimens were embedded in Epon 812 in slide-shaped resin molds (Giammara and Hanker, 1986), and were screened by differential interference contrast (DIC) microscopy and documented in through-focus video vouchers, which were later used to produce measurements for calibrating dimensions of the reconstructed model. After the specimens were reembedded in blocks, serial silver-gold sections (70 nm thick) were taken on a Sorvall (Thermo Scientific, Waltham, MA) MT6000 microtome with a Micro Star (Huntsville, TX) diamond knife. Sections were poststained with methanolic uranyl acetate and lead citrate.

Sections were imaged by using a Philips (Andover, MA) Tecnai T12 transmission electron microscope operating at 120 kV. Images were acquired as montages with a Gatan (Pleasanton, CA) US1000 camera and automatically assembled with DigitalMicrograph (Gatan). Imaging was conducted at the Center for Advanced Microscopy and Microanalysis (CFAMM) at the University of California, Riverside. Brightness and contrast of presented images were adjusted in Adobe Photoshop (San Jose, CA). Ordered images of serial sections were converted to the MRC stack format and manually aligned, individual cell contours were manually traced, and contour-based mesh models of cells were constructed by using the software package IMOD (Kremer et al., 1996). Models were transferred to Blender 2.42 (blender3d.org), an open source ray tracing, mesh modeling, and animation package, for final visualization and production of model figures and animations. All model components visualized herein were reconstructed from a single specimen alignment, except for the anterior tips (~5 μm) of IL1, OL2, CEP1, and CEP2, which were modeled from a composite of two individuals. Four specimens were sampled to check for intraspecific variation. Processing methods, including freeze substitution and infiltration regimens, are described in greater detail in Ragsdale et al. (2008).

Sensory anatomy terminology is consistent with that established for *A. complexus* (Bumbarger et al., 2007), which was based on inferred homologies with cells as named in *C. elegans* (White et al., 1986). Names of cells are thus based on putative homologies with cells in *A. complexus* (and, where applicable, *C. elegans*). Terminology for anterior epidermis in *A. avenae* follows Ragsdale et al. (2008), consistent with that applied earlier to *A. complexus* (Bumbarger et al., 2006). Terminology for anterior cuticular structures of Tylenchomorpha, including *A. avenae*, is derived from Baldwin and Hirschmann (1976).

RESULTS

Reconstruction of the sensory anatomy of *A. avenae* revealed cells that were identified as putative homologs of sensory cells in the nematodes *C. elegans* and *A. complexus*. Hypotheses of homology are based on axial positions of cells, their spatial relationships with adjacent cells, and, where possible, the morphology of their anterior and posterior processes that are distinctive and cell specific in number, structure, and position. The positions of sensory cells relative to the body axis are shown in Figure 1; 3D placement in the head is also shown for individual neurons (Fig. 2) and their support cells (Fig. 3). The cuticular sensilla of the head are partitioned among six similarly sized sectors in a hexaradiate cephalic framework (Fig. 1, 4A,B; see abbreviations list for all figures). By composition, lateral sectors are largely equivalent to one another, as are quadrant sectors. Reconstructions of cuticular sensilla are thus shown from one (subdorsal, left) quadrant (Fig. 4C) and one lateral (Fig. 5A) sector, elucidating differences, where they are apparent, between these sectors within

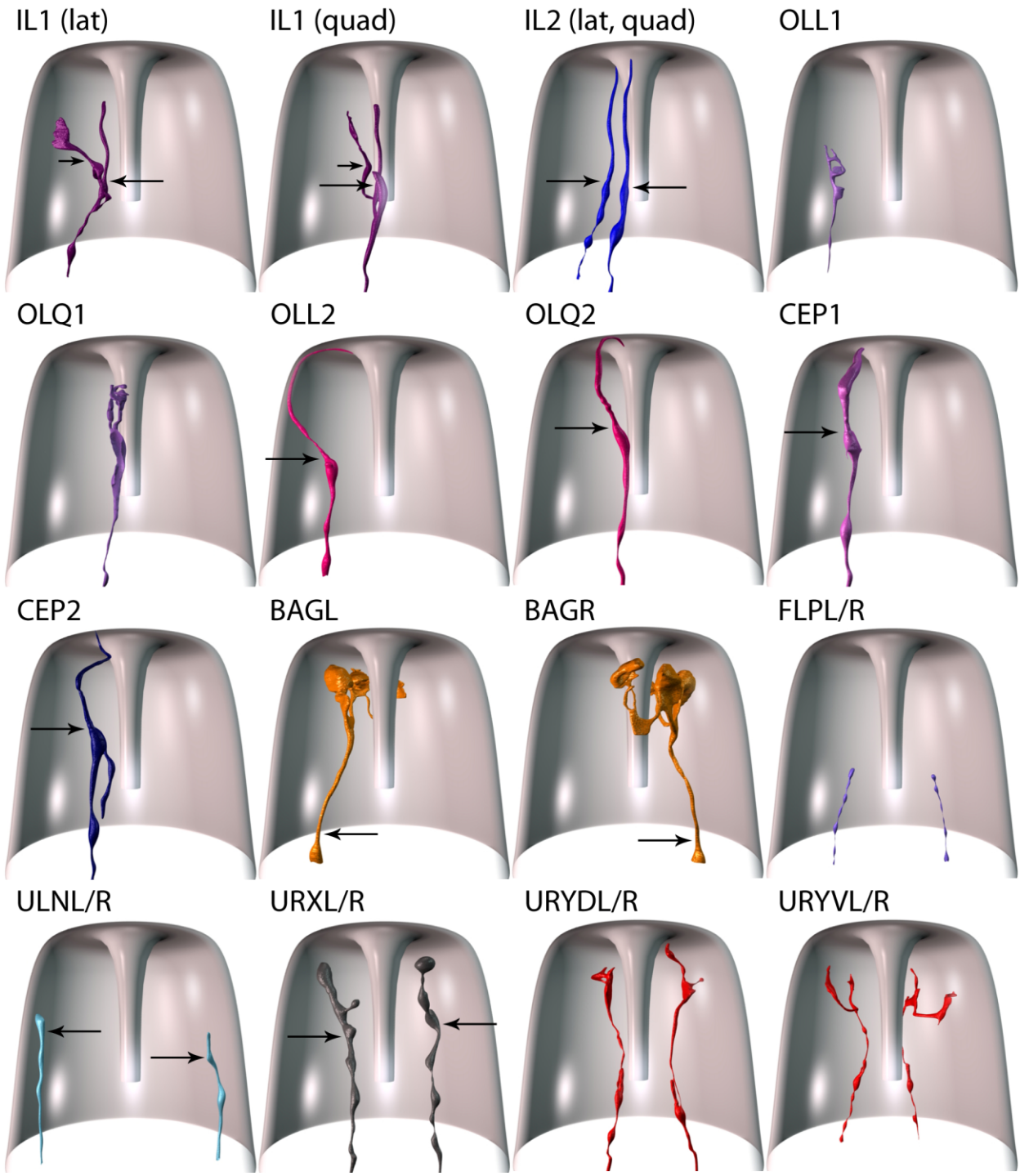

Figure 2.
Individual three-dimensional reconstructions of anterior sensory neurons of *A. avenae*, shown relative to a simplified representation of the anterior body wall cuticle and guiding apparatus. View is dorsal. Quadrant reconstructed is left subdorsal. Cell nomenclature (except for ULN [unnamed lateral neuron]) is consistent with that of White et al. (1986) for proposed homologs of neurons in *C. elegans* (suffixes for internal sensory neurons are: L, left; R, right; D, dorsal; V, ventral). Colors of cells are consistent with key in Figure 5F. Long arrows indicate bases of dendrite cilia; short arrows indicate bases of cilia for accessory processes of IL1. lat, lateral sector; quad, quadrant sector. For other abbreviations, see list.

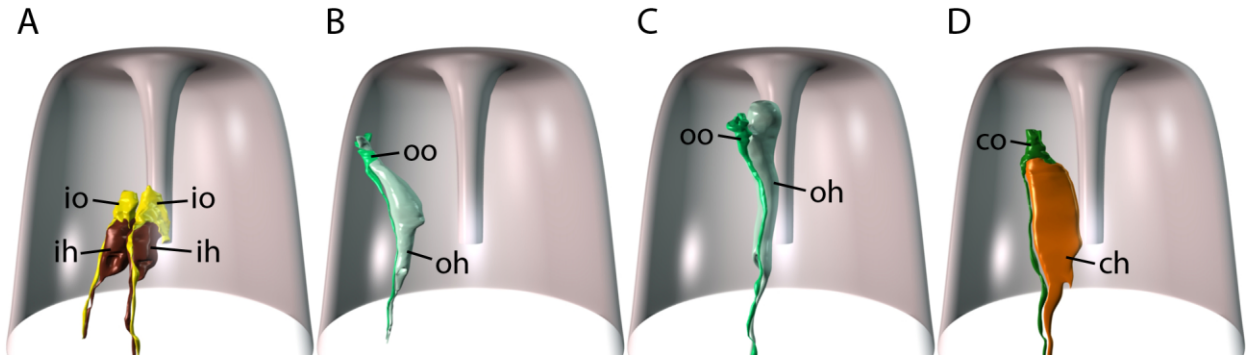

Figure 3.
Reconstructions of support (socket and sheath) cells for individual anterior sensilla of *A. avenae*, shown relative to a simplified representation of the anterior body wall cuticle and guiding apparatus. View is dorsal. Quadrant reconstructed is left subdorsal. Colors of cells are consistent with key in Figure 5F. **A:** Inner labial sensilla of lateral and quadrant sectors. **B:** Lateral outer labial sensillum. **C:** Quadrant outer labial sensillum. **D:** Cephalic sensillum. For abbreviations, see list.

any one class of sensory organ. Internal receptors are shown from all applicable sectors because of variation observed in some cases in left/right and dorsal/ventral symmetry. Cilia have varying numbers of microtubule doublets between and sometimes within types of sensillum dendrites; internal receptor cilia, where present, all show nine doublets encircling two single microtubules. Rootlets were observed in all ciliated dendrites, although they often were not prominent.

Cuticular sensory organs of all five classes penetrate between epidermal syncytia in the anterior end of the nematode and terminate among six lips (two subdorsal, two lateral, and two subventral). Cuticular sensilla include six inner labial sensilla, six outer labial sensilla, four cephalic sensilla, and two amphids (Figs. 1, 4A). In a parallel approach to the corresponding study of *A. complexus*, detailed reconstruction of the amphids of *A. avenae*, which are highly complex relative to other anterior sensory organs, will be presented separately (Ragsdale, in preparation); however, positions of amphid support cells as they relate to other anterior sensory structures are presented herein. Excluding amphids, all cuticular sensilla consist each of two dendrites that enter the sensory channel as well as two support cells, a socket cell, and a sheath cell. Within their corresponding sheath cells, all ciliated sensillum dendrites are swollen at the distal end of their basal body, just proximal to the base of their cilium. Sheath cells also include abundant endoplasmic reticulum, secretory granules, and/or lipid globules. The sensillum socket cells are each positioned between two epidermal syncytia, which are arranged as a series of rings around the stylet and guiding apparatus and underlying the labial and body wall cuticle (Ragsdale et al., 2008). Syncytia HypC and HypE flank the amphid and outer labial socket cells, whereas the inner labial socket cells are embedded between HypB and HypC.

Five classes of internal receptors terminating in the head of the nematode, excluding internal amphid dendrites (Ragsdale, unpublished), were identified: two lateral/subventral BAG dendrites; two lateral/subdorsal URX dendrites; four quadrant URY dendrites; two lateral FLP dendrites; and two "unnamed lateral neurons" ("ULN") (Figs. 4A,B, 5B).

Inner labial sensilla

Each inner labial sensillum has two dendrites that anteriorly penetrate the sheath cell and enter the sensory channel enclosed by the socket cell. The socket cell penetrates between the toroids of HypB and HypC and abuts upon the cuticle of the stylet guiding apparatus (Figs. 4A, 5B,C). The cuticle of the sensory channel joins that of the guiding apparatus, along which both inner labial dendrite cilia lie (Figs. 2, 6A–C); the cuticle-lined cilia are surrounded distally by the HypC syncytium (Fig. 6A–C). The socket cell is an incomplete ring, with its two sides forming a tight junction ("self-junction") where they meet subcuticularly. The first inner labial dendrite (IL1) terminates within the cephalic framework, in its cuticular channel within HypC. The dendrite IL1 enters the sheath cell from the dorsal side in the lateral sensilla, or from the dorsal and ventral sides in the dorsal and ventral quadrant sensilla, respectively. At this point of entry, a process branches from the dendrite and wraps obliquely around the socket cell (posteriad and medially) and sheath cell (anteriad and peripherally) of the sensillum (Figs. 5A, 6B). The loop formed is incomplete at its external end, where both sides approach each other but do not fuse. A variation in symmetry was observed in one specimen, such that the right subdorsal quadrant sensillum has the dorsal branch of the loop crossing to the left side of the body to terminate against the left inner labial socket cell. In several specimens the ventral branch of the left subventral quadrant sensillum extends a process in the toroid of HypC, connecting to it through extensive gap junctions (Fig. 6C).

The medial sides of the IL1 loops are attached to and possibly contain thin-diameter filaments that cross the extracellular space into the cytoplasm of the "wings" of HypB; the filaments are oriented circumferentially, running in a ring around the HypB toroid and guiding apparatus (Fig. 7A,B). The source of these filaments, which are possibly associated with hemidesmosomes, seems to be HypB, but this is unclear from current data. From the anterior end of one branch of each IL1 loop (the dorsal branch in the lateral sensilla, the ventral and dorsal in the dorsal and ventral quadrant sensilla, respectively), a ciliate process extends anteriad and peripherally (Figs. 2, 5A, 6A). The process of each quadrant IL1 runs between the sheath cells and then the socket cells of the quadrant outer labial sensillum and cephalic sensillum, terminating in the pocket of HypC surrounding those socket cells. The flatter process of the lateral IL1 (Figs. 2, 5A, 7C) extends between the sheath and then the socket cell of the lateral

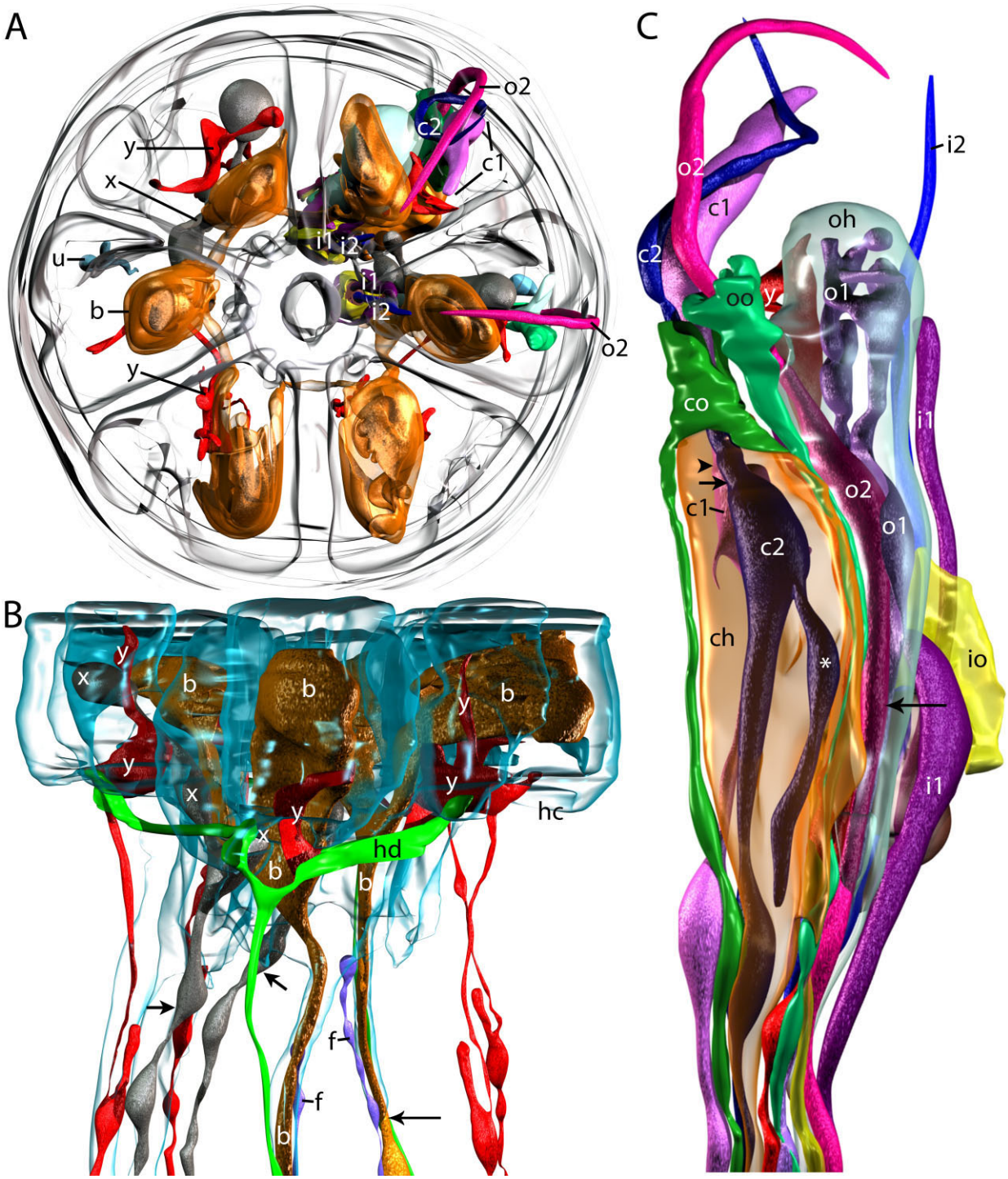

Figure 4.
Three-dimensional reconstruction of anterior sensory structures of *A. avenae* based on serial TEM sections. Color key to cells is given in Figure 5F. Where possible, colors are consistent with those used by Bumbarger et al. (2007). Neurons are rendered with a rough surface texture; arrows indicate bases of cilia. **A:** En face view of all sensory system cells reconstructed herein, with a section of the cephalic framework rendered transparent gray; BAG dendrites are rendered partially transparent to show complex lamellae in their termini. The terminus of CEP1, marked by line brackets, is shown where it reticulates across the quadrant sector toward the body axis; CEP2 is shown terminating in a partial spiral with a peripherally directed tip. Internal receptors on one lateral side and ciliated sensillum neurons are labeled. **B:** Ventrolateral view of internal receptors BAG, FLP, URX, and URY, with termini (except that of FLP) embedded in hexaradiate toroid of epidermal syncytium HypC, which is truncated anteriorly and rendered transparent; a lateral "HypD" cell is displayed in relation to HypC. Long arrow indicates base of BAG cilium and entry of BAG dendrite into pseudosomal extension of HypC; short arrows indicate URX cilia. **C:** Dorsal view of left subdorsal quadrant sensory structures. Sheath cells of the outer labial and cephalic sensilla are rendered transparent to show dendrites within them, including the accessory process (asterisk) of CEP2, a small accessory process near the base of the cilium of CEP1, and terminal branching of OLQ1. Inner labial socket cell is also rendered transparent. Arrowhead indicates CEP1 cilium; short arrow, CEP2 cilium; long arrow, OLQ2 cilium. For abbreviations, see list.

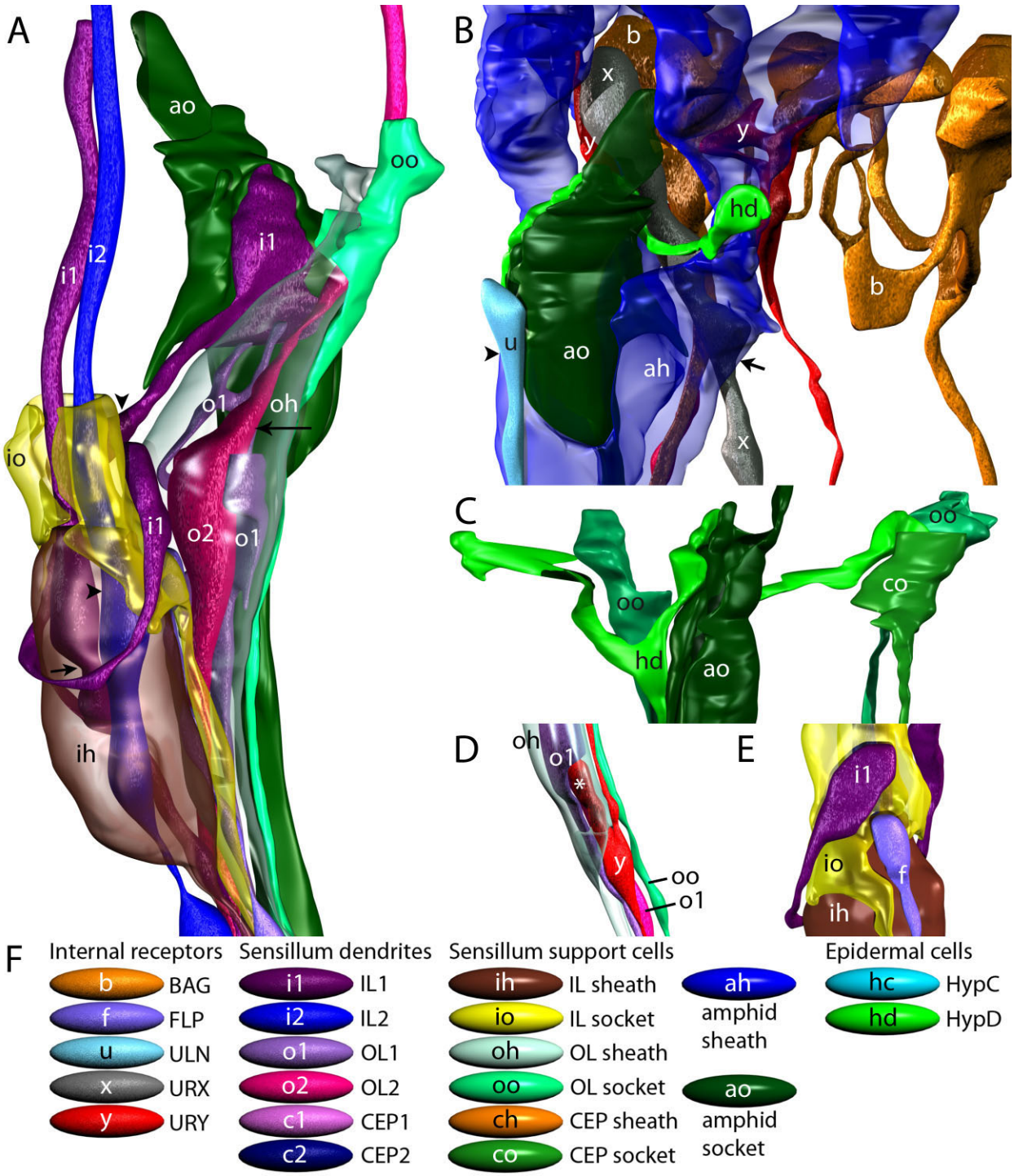

Figure 5.
Three-dimensional reconstruction of anterior sensory structures of *A. avenae* based on serial TEM sections. Where possible, colors are consistent with those used by Bumbarger et al. (2007). Neurons are rendered with a rough surface texture; arrows indicate bases of cilia. **A:** Ventral and medial (to body axis) view of lateral sector sensory structures with sheath cells of the inner labial and outer labial sensilla rendered transparent to show dendrites within them, including terminal branching of OLL1; inner labial socket cell is also rendered transparent. Positions of cells, including the wing-like extension of IL1, are shown relative to the amphid socket cell. The medial loop of IL1 is shown wrapping around the inner labial support cells. Short arrow indicates IL1 cilium; vertical arrowhead, cilium of IL1 accessory process; horizontal arrowhead, IL2 cilium; long arrow, OLL2 cilium. **B:** Dorsal and distal (to body axis) view of internal receptors, shown in relation to the amphid socket (transparent) and sheath (slightly transparent) cells; position of "HypD" is also shown. Internal receptors are seen through (not within) amphid support cells. Arrowhead indicates ULN cilium; short arrow, URX cilium. **C:** Lateral view of quadrant and lateral socket cells of the amphid as well as outer and cephalic sensilla, positions of which are shown relative to HypD. **D:** Lateral and distal view of quadrant outer labial sensillum with process (asterisk) of URY within the sheath cell. **E:** Lateral and distal view of inner labial sensillum, showing incomplete loop of IL1 and association of the FLP terminus with the sensillum. Inner labial socket cell is rendered transparent. **F:** Key to cells in Figures 2–5. Cell name abbreviations are consistent with those used in text. For abbreviations, see list.

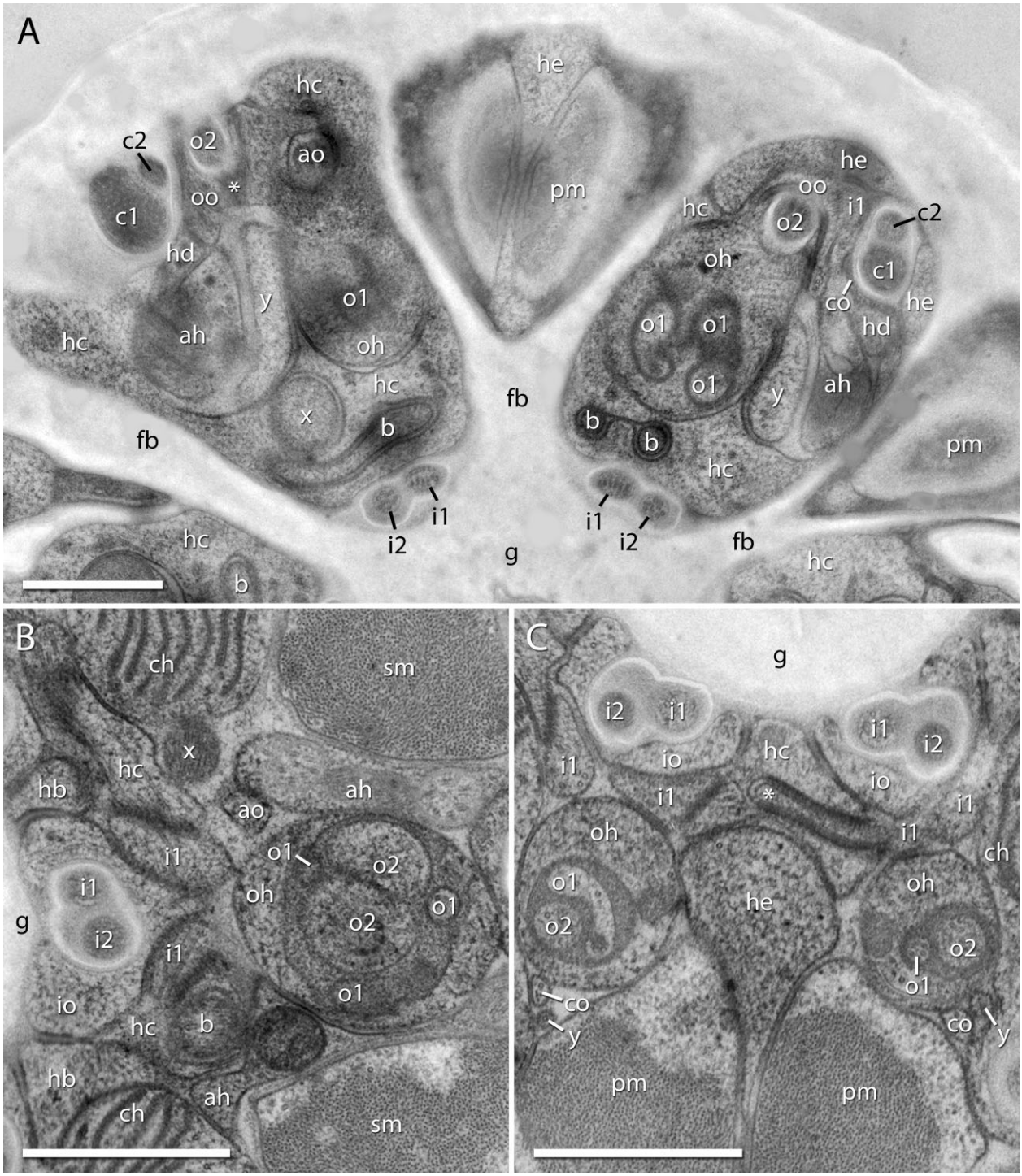

Figure 6.
Transverse TEM sections of anterior sensory structures of *A. avenae*. Adjacent epidermis, muscles (somatic and stylet protractor), and cuticular structures are also shown. Top of page is dorsal. **A:** Slightly oblique section through subdorsal, quadrant sectors of sensory structures and associated epidermal cells and syncytia within cephalic framework (comprised of guiding apparatus and framework blades). Internal receptors BAG, URX, and URY terminate within pockets of HypC. The anterior swelling quadrant outer labial sheath cell is shown with internally branching OL1. The medial self-junction of the outer labial socket cell is shown in oblique section (asterisk). The wing-like process of IL1 extends between the outer labial and cephalic socket cells. CEP dendrites meet body wall cuticle (shown left in figure) just posterior to crossing HypC transversely. Transverse strands of "HypD" also connect to outer labial and cephalic socket cells. **B:** Lateral sensory structures posterior to the framework. Cilium of BAG is within pseudosomal extension of HypC; the cilium of URX is free (shown anterior to being enveloped by the cephalic sheath cell and posterior to its entry into HypC). The accessory process of IL1 is shown at the distal, anterior end of its incomplete loop around the inner labial support cells. The fine branches of OL1 surround the swollen basal body of OL2 (with minor bifurcation) within the outer labial sheath cell. **C:** Ventral sensory structures just posterior to the framework, at the same transverse position shown in Figure 6B. The process (asterisk) of the accessory loop of left, subventral IL1 terminates within HypC, connecting through gap junctions. For abbreviations, see list. Scale bar = 1 μm in A–C.

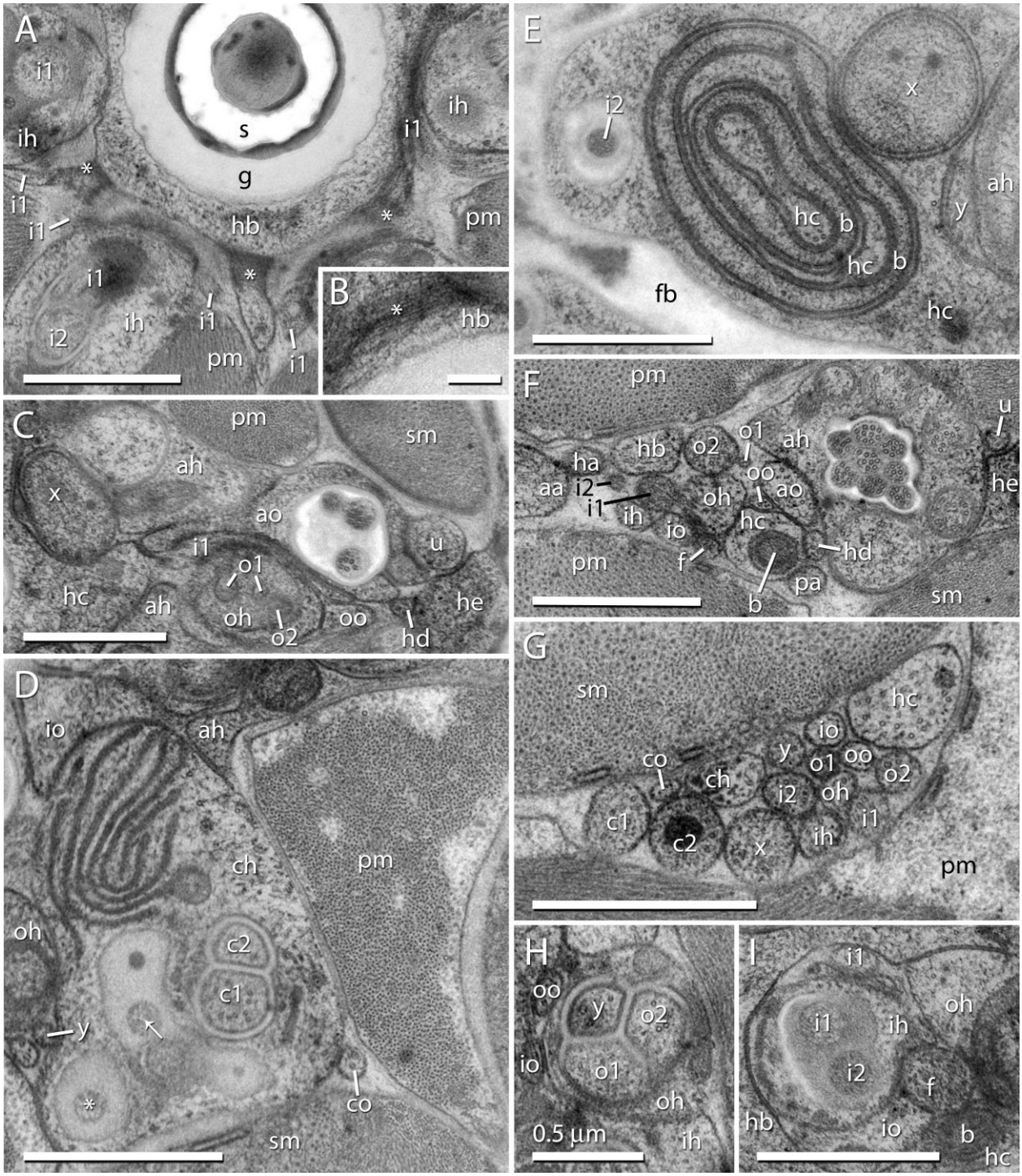

Figure 7.

Transverse TEM sections of anterior sensory structures of *A. avenae*. Adjacent epidermis, muscles (somatic and stylet protractor), and cuticular structures are also shown. Top of page is dorsal. **A:** Ventral and lateral sensory structures around posterior end of stylet guiding apparatus. The accessory processes of IL1 are shown at their internal, posterior end of their incomplete loops around their respective inner labial support cells. Thin-diameter filaments (asterisks) that apparently originate from the accessory loops of IL1, cross the extracellular spaces to the "wings" of the HypB toroid, which they span to form a "ring" around the guiding apparatus and stylet. **B:** Filaments (asterisk) within "wing" of HypB toroid. **C:** Lateral sensory cells at a position between those of Figure 6A,B and the cephalic framework. The cilium of URX is swollen, shown just posterior to its branching and entry into HypC. The wing-like process of the IL1 accessory loop extends between amphid and outer labial support cells. Unnamed lateral neuron connects to amphid socket cell. The somal extension of "HypD" is shown posterior to its transverse extensions. **D:** Cephalic sensillum and adjacent subventral cells at the level of the posterior end of the guiding apparatus. Asterisk marks the prominent, posterior accessory process of CEP2; arrow indicates one of a few minor cell processes of CEP2 (not consistently present across individual CEP neurons). **E:** Lateral sector within framework showing lateral branches of URX and URY as well as multiple terminal lamellae of BAG within HypC. **F:** Lateral bundle of sensory, epidermal, and arcade cell processes. The cilium of BAG is shown just anterior to its entry into the pseudosomal extension of HypC, at a level posterior to the framework and guiding apparatus. **G:** Subventral process bundle, at a level posterior to the framework and guiding apparatus. **H:** Posterior part of quadrant outer labial sheath cell, including accessory process of URY, at a level immediately posterior to the guiding apparatus. **I:** Connection of FLP terminus, with dense cytoplasm, to inner labial sheath cell, at the level of the guiding apparatus, just posterior to the framework. For abbreviations, see list. Scale bar = 1 μm in A, C–G,I; 0.2 μm in B.

outer labial sensillum and the amphid socket cell, terminating with a process in the latter. The second inner labial dendrite (IL2) has a cilium that extends to the surface of the labial cuticle, where it terminates in an opening to the external environment (Figs. 4C, 5A). In the inner labial sheath cells, internal membranous lamellae and large lipid globules are common. No accessory dendrites associated with the inner labial sensilla were observed.

Outer labial sensilla

The outer labial sensilla each have two dendrites that enter the sensory channel, with the quadrant sensilla sheath cells also enclosing a process of URY posteriorly. The first outer labial dendrite (OL1), which lacks a cilium, terminates within the sheath cell. The terminus of the dendrite is highly branched (Figs. 2, 4C, 5A, 6A,B, 7C), sometimes appearing multilamellar. The primary bifurcation of OL1 is at the junction between the sheath and socket cells, although further anterior branching is variable. Posterior to this branching, OL1 partially wraps around the second outer labial dendrite (OL2) within an electron-dense matrix (Fig. 6C), especially where the latter swells within the sheath cell (Figs. 4C, 5A). The terminal branches of OLQ1 are more greatly expanded anteriorly than are those of OLL1. Correspondingly, the quadrant outer labial sheath cell extends and remains swollen anterior to its connection to the socket cell (Fig. 4C), accommodating OLQ1 as well as most of the observed secretory products of the sheath cell. The sheath cell of each lateral outer labial sensillum is comparatively small (Fig. 5A), without an anterior swelling, and with a minimal amount of secretory products in the cytoplasm. Internal membranous lamellae are absent in all outer labial sheath cells.

Dendrite OL2 is generally simple in morphology (Fig. 2). In some cases, OL2 has a small process in the sheath cell in addition to the main, axial dendrite that emerges anteriad from the sheath cell (Fig. 4C). The cilium of OL2 enters the cuticle-lined duct in the socket cell, from which it enters the body wall cuticle at the base of the lip, midway between the blades of the framework that define each lip. The terminus of the dendrite extends anteriad, unbranched, through the labial cuticle (Fig. 2) and ends within the cuticle a short distance from the IL1 terminus of the same sector (Fig. 4A,C).

The socket cell meets the labial cuticle between HypC (anteriorly) and HypE (posteriorly), forming a self-junction at the side opposite the dendrite from the cuticle (Fig 6A). A pair of minor, apparently epithelial cells that do not line the cuticle (henceforth designated as "HypD") extend in small strands transversely from their lateral axial positions. These cells contact all three outer labial socket cells on their corresponding sides (Figs. 5B,C, 6A). The transverse strands of these cells terminate dorsally and ventrally where they meet the socket cells.

Cephalic sensilla

The two cephalic dendrites, CEP1 and CEP2, enter the sensory channel through the sheath cell (Fig. 7D). Within the sheath cell, CEP2 has a distinct, posteriorly directed accessory process that separates from the main sensory channel bundle (Figs. 4C, 7D). The process runs along the sagittal and distal margin of the sheath cell, persisting posteriad to about the point of entry of the dendrites into the sheath cell (Fig. 4C). Additional minor accessory processes are variably present near the basal bodies of CEP1 and CEP2 within the sheath cell (Figs. 4C, 7D). The sheath cell of the cephalic sensillum is by far the most prominent among the anterior sensory organs (Fig. 3), with also the most extensive internal lamellae (Fig. 7D).

The cilia of both CEP1 and CEP2 enter the socket cell and ultimately the cuticle. The narrow cephalic socket cell, like that of the outer labial socket cells, is anchored between HypC and HypE, but also contacts strands of "HypD" (Figs. 5C, 6A). Both dendrites enter the body wall cuticle at the base of the lip. Anterior to joining the body wall cuticle, CEP1 extends inward toward the body axis (Figs. 2, 4C), crossing its corresponding quadrant sector of HypC in the cephalic framework but still enclosed by cuticle. Its terminus is unbranched, swollen (Figs. 5C, 6A), and filled with microtubules and particularly osmophilic material (Fig. 6A), terminating blindly just beneath the labial cuticle. The terminus of CEP2 turns centrally, initially parallel to CEP1, but then in one turn of a spiral directs peripherally again (Figs. 2, 4A,C) and terminates in a papilla with an opening to the external environment.

Internal sensory receptors

Five classes of internal sensory neurons were observed terminating in the head of *A. avenae*. Four classes were assigned putative homologies with respect to *C. elegans* and *A. complexus* (BAG, URX, URY, and FLP); one class ("ULN") is of unknown homology.

The two BAG dendrites (Figs. 2, 4A,B, 6A,B, 7E) are the most prominent of the internal receptors, both axially and at their termini. They are located subventrally in the lateral bundles of neurons and syncytial somal extensions. The cilium of each dendrite is enveloped by one of two long pseudosomal extensions of HypC (Figs. 4B, 7F). The ciliary region of the dendrite persists anteriorly to a point at which the pseudosomal extension joins the main body of the HypC toroid. At the level of the toroid proper, the pair of cilia branch and expand to comprise a multilamellar complex that fills much of HypC, connecting to it by gap junctions, in all six sectors of the cephalic framework (Figs. 4B, 7E). Termini of both dendrites are adjacent in some sectors; their individual lamellae fold around each other, but they do not fuse. In at least one specimen (the model reconstructed herein), the complex of the two dendritic termini seems to be discontinuous across the right lateral and right subdorsal sectors. It is not clear whether the precise distribution of terminal branches among sectors is conserved across nematode individuals.

The URX dendrites are axially subdorsal (Figs. 1, 4A, 7G), most consistently associated with the subdorsal cephalic sheath cells. Where the cephalic sheath cell expands around its sensory channel, it also envelops URX, which extends toward a more lateral axial position (Fig. 6B). The cilium of URX is anterior to its associated cephalic sheath cell, near to where it becomes embedded in the HypC toroid (Fig. 7C). Upon entering the HypC toroid, by way of gap junctions, the URX cilium splits into both a lateral and subdorsal branch, which terminate blindly within the corresponding sectors of HypC (Figs. 4B, 6A, 7E).

The four URY dendrites are distributed among the subdorsal and subventral process bundles (Fig. 7G), most consistently in proximity to the cephalic sheath cell. Where the quadrant outer labial dendrites enter their sheath cell, the URY swells and branches into an accessory process in contact

with the former dendrites in their sensory channel (Figs. 5D, 7H). The accessory process extends only a fraction of the longitudinal distance of the sheath cell before terminating. In each quadrant, the main dendritic process is associated with a branch of the corresponding amphid sheath cell that enters that quadrant (Figs. 5B, 6A). Each subventral URY dendrite also branches transversely into the adjacent lateral sector, where it contacts the lateral part of the amphid sheath cell (Figs. 5B, 6D). The dorsal URY cells, by contrast, do not have branches extending to the lateral sectors (Fig. 2). The URY dendrites terminate anteriorly in pockets of HypC, together with the amphid sheath cell, in the cephalic framework; they are variably branched at their absolute termini (Figs. 2, 4A,B). No cilia are observed in URY.

The putatively assigned FLP dendrites are located in the lateral pseudocoelomic cords (Fig. 7F), close to the outer labial sheath and inner labial sheath and socket cells. Their termini are slightly swollen with dense cytoplasm (Fig. 7I) but are otherwise unspecialized, lacking a cilium, and ending deep within the nematode head (Figs. 2, 4B). The terminus connects anteriorly to a small pocket of the inner labial socket cell, just anterior to the sheath cell (Figs. 5E, 7I).

Each of the two unnamed lateral neurons are located laterally and peripherally in the body, between the lateral epidermal cord (HypE anteriorly, both HypE and HypF posteriorly), somatic muscle dorsally, and, for much of its anterior length, the amphid medially (Fig. 7C,F). Each unnamed lateral neuron is simple in morphology, with a short cilium beginning closely posterior to where it terminates in a shallow indentation of the amphid socket cell (Fig. 7C).

DISCUSSION

Reconstruction of the anterior sensory anatomy of *A. avenae* shows a high degree of conservation of sensory structures with freeliving Rhabditida nematodes. Novel, detailed modeling shows that several aspects of sensory morphology and connectivity share a persuasive degree of similarity between representatives of Cephalobomorpha and Tylenchomorpha. Furthermore, extensive similarity with even the distant outgroup *C. elegans* allows identification of homologies necessary for extending testable models of nervous system function. Complete reconstruction of anterior cuticular sensilla and other sensory neurons in *A. complexus* (Bumbarger et al., 2007) and *C. elegans* (Ward et al., 1975; White et al., 1986) allows a detailed, comparative approach with corresponding results for *A. avenae* presented herein (Table 1). Conservation of morphology and, to a great extent, axial position of sensory cells (Fig. 1) facilitates reliable assessments of homology. In spite of its disparate feeding styles with respect to other models examined, *A. avenae* shares a remarkable amount of conservation in its anterior sensory system, corroborating that previously shown between *A. complexus* and *C. elegans* (Bumbarger et al., 2007). Knowledge of numbers, positions, and relative orientation of sensory cells in *A. avenae* builds upon previous knowledge of tylenchid sensory anatomy to extend homology proposals throughout Tylenchomorpha.

In addition to establishing a functional systems model of a tylenchid nematode, TEM reconstruction of the anterior sensory anatomy offers an alternative source of evidence important for phylogeny, namely, to resolve the position of Tylenchomorpha relative to freeliving outgroups. The present work demonstrates that, in contrast to characters traditionally important in Rhabditida taxonomy, the level of conservation of sensory characters is suitable for resolution of deep level relationships within the group. Implications of reconstruction results for systematics of Rhabditida will serve as a test of congruence between morphology and molecular sequence data, to be presented separately (Ragsdale, in preparation).

Comparison with freeliving outgroups: cuticular sensilla

Inner labial sensilla. In *A. avenae* and both freeliving outgroups, the inner labial sensilla are characterized by having two dendrites, one of which (IL1) terminates within the sensory channel of the socket cell, proximal to the exterior opening of the sensillum. However, IL1 differs substantially in both *A. avenae* and *A. complexus* relative to *C. elegans* in having a prominent accessory process that branches just proximally to the cilium and wraps around the internal margin of the sheath cell. In *A. avenae*, the process also extends to encircle the support cells at their external margin, although it does not form a complete ring. Unique to IL1 of *A. avenae* is an additional ciliate process that extends from the loop-like accessory process to associate with the support cells of other sensilla. In contrast to the relatively elaborate morphology of IL1 in *A. avenae* and *A. complexus*, this neuron in *C. elegans* has no process other than the ciliate terminus of the dendrite.

In *A. complexus*, filaments extending from IL1, through HypB, and connecting distally to the cuticle of the probolae and stoma lining were postulated as comprising a "new type of receptor," perhaps detecting stretching of the labial cuticle such as by expansion of the stoma (Bumbarger et al., 2007). This configuration is not seen in *A. avenae*. However, the cuticle forming the probolae in *A. complexus* is homologous with that of the guiding apparatus in *A. avenae*, as inferred from the position of HypB, the corresponding, underlying epidermis (Ragsdale et al., 2008). Interestingly, where HypB encircles the guiding apparatus, filaments that appear to originate in the accessory processes of IL1 instead span the compressed "wings" of HypB. These filaments to do not attach to the cuticle but instead form a ring around the guiding apparatus, possibly fostering mechanical communication between individual sensilla. Stretching of the guiding apparatus, as would occur upon protrusion of the tapered stylet, might uniformly pull upon all IL1 accessory processes in a manner that converts the processes into simultaneous stretch detectors. An alternative explanation for this band of filaments is that it is purely mechanical, to aid in guiding the stylet. Although possible roles of the filaments are still speculative, any functional association of IL1 with HypB (Hyp2 in *C. elegans*) would be uniquely shared between *A. avenae* and *A. complexus* with respect to examined outgroups, including *C. elegans*, the strongylid (Rhabditomorpha) Nippostrongylus brasiliensis (Wright, 1975), and the filariid Onchocerca volvulus (Strote and Bonow, 1993).

General function of the structurally simple IL2 dendrite as a chemoreceptor is conserved in all nematodes examined. In contrast to both outgroups, no "accessory neurons" associated with the inner labial sheath cells (Ward et al., 1975; Bumbarger et al., 2007) were observed in *A. avenae*; the questionable homology of these cells or cell processes with respect to Tylenchomorpha remains unresolved.

TABLE 1. Presence and Characteristics of Homologous Anterior Sensory and Associated Cells in *Aphelenchus avenae*, *Acrobeles complexus*, and *Caenorhabditis elegans*

Cell name	Cell description (no. of cells) Distinctive characteristics	*A. avenae*	*A. complexus*	*C. elegans*
IL1	**Inner labial dendrite 1 (6)**	+	+	+
	Ciliated terminus	+	+	+
	Mechanoreceptive	+	+	+
	Accessory partial loop	+	+	–
	Contact with HypB/Hyp2	+	+	–
	Left ventral IL1 with process in HypC	+	–	–
	IL1 process filaments through HypB	+	+	–
	Filaments proximal to cuticle:	+	+	?
	In ring around stoma cuticle	+	–	?
	Attaching to cuticle	–	+	?
	Second ciliate process	+	–	–
IL2	**Inner labial dendrite 2 (6)**	+	+	+
	Ciliated terminus	+	+	+
	Chemoreceptive	+	+	+
	Simple, unbranched terminus	+	+	+
	Inner labial sheath cell (6)	+	+	+
	Inner labial socket cell (6)	+	+	+
	Ring formed by self-junction	+	+	+
	Inner labial accessory neuron (2–4)	–	+ (4)	+ (2)
OL1	**Outer labial dendrite 1 (6)**	+	+	–
	Ciliated terminus	–	–	N/A
	Terminus within sheath cell	+	+	N/A
	Terminus bifurcate	+	+	N/A
	Extensive branching within sheath cell	+	–	N/A
	OLQ1 more expansive than OLL1	+	–	N/A
	Wraps around OL2	+	–	N/A
OL2	**Outer labial dendrite 2 (6)**	+	+	+
	Ciliated terminus	+	+	+
	Mechanoreceptive	+	+	+
	OLQ branching outside sheath cell	–	+	–
	Terminus with “nubbin” in cuticle	–	–	+
	Outer labial sheath cell	+	+	+
	Internal membranous lamellae	–	+	+
	Outer labial socket cell	+	+	+
	OLQ socket swollen compared with OLL	+	–	–
	OLQ sockets surround CEP cilia	–	+	–
	Ring formed by self-junction	+	+	+
CEP1	**Cephalic dendrite 1 (4)**	+	+	+
	Ciliated terminus	+	+	+
	Mechanoreceptive	+	+	+
	Blind, swollen terminus	+	+	+
	Terminus with “nubbin” in cuticle	–	–	+
	Prominent accessory process	+	–	–
CEP2	**Cephalic dendrite 2 (4)**	+	+	+ (CEM)
	Ciliated terminus	+	+	+
	Chemoreceptive	+	+	+
	Presence in female/hermaphrodite	+	+	–
	Cephalic sheath cell (4)	+	+	+
	Internal membranous lamellae	+	+	+
	Cephalic socket cell (4)	+	+	+
	Ring formed by self-junction	+	+	+
BAG	**BAG sensory neuron (2)**	+	+	+
	Ciliated terminus	+	+	+
	Cilium with prominent rootlet	+	+	+
	Cilium = 9 doublets + 2 singlet MTs	+	+	+
	Associated with epidermis	+	+	+
	Base of cilium enters HypC/Hyp3	+	+	+
	Extensive multilamellar terminus	+	+	–
	Terminus in quadrant sectors	+	+	–
FLP	**FLP sensory neuron (2)**	+	+	+
	Ciliated terminus	–	–	+
	Connects to IL socket	+	–	+
	Penetrates HypB	–	+	–
	Extensive branching of dendrite	–	–	+
URX	**URX sensory neuron (2)**	+	+	+
	Ciliated terminus	+	+	–
	Branched terminus	+	+	–
	Terminus in HypC	+	+	–
	Process terminating in amphid socket	+	+	–
	Posteriad, lateral arm	–	+	–
	Accessory process proximal to cilium	–	+	N/A
URY	**URY sensory neuron (4)**	+	+	+
	Ciliated terminus	–	–	–
	Branched terminus	+	+	+
	Association with BAG	–	+	–
	Accessory process in OLQ sheath cell	+	–	–
	Association with amphid support cell:	+	+	?
	Amphid sheath	+	–	?
	Amphid socket	–	+	?
	Dorsal pair with lateral extensions	–	+	?
–	**Unnamed lateral neuron (2)**	+	URX arm?	? (see text)
	Ciliated terminus	+	?	?
	Terminates at amphid socket	+	?	?
	Runs between Hyp cord and amphid	+	?	?
HypD	**Epidermis cell D (2)**	+	+	–
	Lines IL, OL, and amphid sockets	+	+	–
	Pair of cells forming a syncytium	–	+	N/A

For abbreviations, see list.

Outer labial sensilla. Two dendrites comprise each outer labial sensillum of both *A. avenae* and *A. complexus*. In *C. elegans* only one (OLL or OLQ, in lateral and quadrant sensilla, respectively) is present. Based on its conserved, simple expression, this neuron was considered homologous with what was named "OL2" (OLL2 and OLQ2) in *A. complexus* (Bumbarger et al., 2007). The dendrites OLL1 and OLQ1 (collectively OL1), homologies of which are not known in *C. elegans*, lack a cilium and terminate in their sheath cells in both *A. avenae* and *A. complexus*. The terminus of OL1 in *A. avenae* is unique in being highly and irregularly branched within the sheath cell, whereas in *A. complexus* a single bifurcation is observed. The distinct wrapping of OL1 around OL2 in a dense matrix, not observed in *A. complexus*, may indicate some enhanced interaction between the two dendrites. The possible function of such an elaborate, bare terminus is elusive. Conversely, OLQ2 in *A. complexus* is highly branched outside of the support cells, whereas none of the OL2 dendrites have external accessory processes in *A. avenae*.

A feature conserved with both outgroup taxa is the relationship of OL2 to the labial cuticle as a mechanoreceptor, probably involved in nose touch response (Hart et al., 1995; Bumbarger et al., 2007). However, as in *A. complexus*, the OL2 terminus of *A. avenae* lacks the additional "cuticular nubbin" described for *C. elegans* (Perkins et al., 1986). In *A. avenae*, the cilia of both OLL2 and OLQ2 each extend through the apex of a lip. The coordination between this touch response and "foraging" behavior would be significant in a plant parasite or fungal feeder, which, for mechanical reasons, establishes contact between all lip apices and the root or hypha of its host before injecting its stylet to feed (Dickinson, 1959; Fisher and Evans, 1967). The association of the quadrant outer labial socket cell with the "sensory channel" of the cephalic sensillum is not observed in *A. avenae* as it is in *A. complexus*, nor is there the possibly related discrepancy in size between quadrant and lateral socket cells.

Cephalic sensilla. In contrast to *C. elegans*, both *A. avenae* and *A. complexus* also have two ciliated cephalic dendrites. Like its proposed homolog CEP in *C. elegans* (Bumbarger et al., 2007), CEP1 of *A. complexus* and *A. avenae* enters and terminates within the cuticle and is presumably mechanoreceptive. It is conserved in being swollen and highly osmophilic; as in *A. complexus*, it lacks an accessory nubbin in the cuticle. In *C .elegans*, CEP1 shows a direct response to the mechanical stimuli of bacterial lawns, which results in slowed locomotion (Sawin et al., 2000). Analogous functions in a migrating plant parasite or fungal feeder, such as contact with host parts, can only be speculated on. The second cephalic dendrite of *A. avenae* and *A. complexus*, CEP2, which has a simple terminus that ends in an open pore, is absent in hermaphrodites of *C. elegans*. It was proposed to be the homolog of CEM (Bumbarger et al., 2007), which is also a chemosensory neuron but is exclusive to *C. elegans* males (Ward et al., 1975).

HypD: an additional epithelial anchor for socket cells. Associated with the socket cells of the outer labial and cephalic sensilla (and amphids) in *A. avenae* is an additional pair of lateral cells, putatively named "HypD." Based on their spatial relationships to the sensilla and their apparently conserved axial positions, these cells are proposed to be, collectively, the homolog of the syncytium HypD of *A. complexus*. The syncytium, characterized by a thin, incomplete toroid and two nuclei, is unique to *A. complexus* among examined taxa. HypD lacks an identifiable homolog in *C. elegans* (Bumbarger et al., 2007).

Comparison with freeliving outgroups: internal sensory receptors

Internal sensory receptors. Internal receptor neurons have the most variable termini between outgroup taxa, constituting greater possible divergence in function. However, despite characters unique to each nematode model, *A. avenae* and *A. complexus* share several peculiar, exclusive similarities in these neurons, allowing reliable statements of homology.

BAG. A prominent similarity between *A. avenae* and *A. complexus* is in the pair of BAG dendrites, characterized by extensive termini branching into multiple lamellae throughout the cephalic framework within HypC (Hyp3 in *C. elegans*). In *C. elegans*, the neurons each simply have a slightly flattened, relatively unspecialized terminus, each ending only in its corresponding lateral sector in associated with the epidermis (White et al., 1986). The shared feature of elaborate branching in the former two taxa, which was recognized as a putative homology based on its general morphology and on HypC epidermis homology (Bumbarger et al., 2007; Ragsdale et al., 2008), is now confirmed by multiple features of axial and terminal position and relationships to neighboring cells. The base of the cilium in both *A. avenae* and *A. complexus* is also conserved in its point of entry into the channel of the corresponding lateral/subventral extension of the HypC toroid. In both taxa, the regular pattern of the cilium is only observed through where these extensions posteriorly join the body of the HypC toroid proper, after which the dendrite branches into its specialized terminus.

The structure of the BAG cilium itself in *A. avenae* is clearly conserved, with both outgroups in having nine doublets surrounding a pair of singlet microtubules as well as a prominent rootlet. Although the exact pattern of branching in the terminus among sextiles in the framework is not clearly shown to be identical across individuals, a shared feature between at least the completely reconstructed models of *A. avenae* and *A. complexus* is a discontinuity in the left, subdorsal "composite" terminus of the two dendrites. However, this apparent conserved asymmetry requires further sampling to test for variation. The structure of the BAG termini has been suggested to be analogous to the highly modified, olfactory amphid wing cells (AWA, AWB, and AWC), by virtue of their extensive, internal surface area (Bumbarger et al., 2007). The type and degree of terminal specialization observed in *C. elegans* wing cells is lacking in possible homologs of *A. complexus* (Bumbarger et al., 2009) and *A. avenae* (Ragsdale, unpublished data), congruent with the suggestion that modified BAG cells may also have assumed an important olfactory role (Bumbarger et al., 2007).

URX and unnamed lateral neurons. The two URX dendrites are positioned generally between the cephalic sheath cells and amphids in all observed taxa (Fig. 1); in at least *A. avenae* and *A. complexus*, they are more closely associated with the former. However, in contrast to *C. elegans*, URX has a cilium and splits into multiple processes in both *A. avenae* and *A. complexus*. Also, in these two taxa, the ciliate processes of URX have branches terminating in pockets of the

amphid socket cell. An accessory process proximal to the cilium, as described for *A. complexus*, is absent in *A. avenae*. The lateral, posterior arms of URX in *A. complexus* are also lacking in *A. avenae*.

Interestingly, another pair of dendrites ("ULN") in *A. avenae* occupies the exact axial position of these arms, including their spatial relationships to neighboring cells (epidermal cord and dorsolateral somatic muscle). In *A. complexus* the "puzzling" lateral arms of URX could not be traced to their posterior ends, and it is possible that these may extend to cell bodies, in which case they would be a case of syncytial dendrites. Near the branching of URX in *A. complexus*, the posterior arm notably runs adjacent to the unciliated branch of URX for some distance before their fusion, which is also unusual for single dendrites. The association of URX with the amphid socket cell in *A. complexus* is comparable to that of the ULN terminus in *A. avenae*, suggesting the possibility of conserved association, despite the lack of connections between URX and ULN in *A. avenae*. A function of URX in *C. elegans* is oxygen sensation, particularly in the pseudocoelomic fluid (Gray et al., 2004; Cheung et al., 2005; Chang et al., 2006), possibly as part of a network with other oxygen sensors (AQR, PQR) to compare oxygen levels across the body (Rogers et al., 2006). If this function is conserved, the extensive junctions of the terminal branches of URX to the toroid of HypC, as observed in *A. avenae*, may indicate greater sensitivity to external stimuli. It is possible that the embedded termini assess ambient oxygen encountered as it diffuses directly into the anterior epidermis. Given the well-characterized signal transduction pathways with URX in *C. elegans*, the morphological divergence of these neurons marks an interesting avenue for further experimental research.

Several candidates for homologs of ULN based on the nervous anatomy of *C. elegans* (White et al., 1986) can be speculated on. Based on similarity of axial position, one candidate is ALM, which is a lateral pair of neurons that also extend along the dorsal edge of the lateral hypodermal cords, are closely apposed to the cuticle, and are mechanoreceptive (Chalfie and Thomson, 1982), but that only extend to the base of the pharyngeal procorpus. However, the prominence of microtubules signifying a similarity in function with ALM was not observed in *A. avenae*. Another possibility for homology with *C. elegans* is the pair of lateral URB interneurons, which in *C. elegans* are not ciliated and taper near the base of the stoma without terminal specializations. However, similarity in axial position is only approximate, as URB lie in the lateral nerve bundles, a position internal to that observed in *A. avenae*.

A third candidate for homology of ULN is AUA. Although AUA of *C. elegans* lacks a cilium, the proposed homolog of AUA in *A. complexus* and *Strongyloides stercoralis* (Ashton et al., 1995), ASA, has a "degenerate" cilium similar to that of ULN in *A. avenae*. Homology with AUA would include the possibility of sharing characterized functions in social feeding behavior (Coates and de Bono, 2002), a prospect with interesting implications for a plant parasitic lifestyle. In the case of homology with AUA, the possibility of homology of ULN with the posterior "extension" of URX in *A. complexus* would necessarily be rejected. Testing this possibility will require complete reconstruction of the amphid of *A. avenae* (Ragsdale, in preparation).

URY. The URY dendrites of *A. avenae* are similar to those of both model outgroups in lacking cilia and terminating in pockets in the anterior epidermis that is definitely HypC in *A. avenae* and *A. complexus*. The elaborate terminal branching, although less extensive in *A. avenae* than in *A. complexus*, also seems to be a shared feature among all three examined taxa, with branching in *C. elegans* informed by confocal fluorescence microscopy (Aronoff et al., 2004). Differences in branching in *A. avenae* with respect to *A. complexus* are the general but not complete lack of prominent posterior projections, their lateral extensions in the subdorsal pair, and their association with BAG. The association of the terminal branches of URY with the anterior projections of the amphid sheath is peculiar to *A. avenae*. Although this configuration is precluded in *A. complexus* by the lack of such projections of the amphid sheath cell (Bumbarger et al., 2009), the lateral, posterior branch processes of URY are in contact with the amphid socket cell. Shared association of URY with an amphid support cell in both nematodes may indicate a loosely conserved connectivity to the sensillum or its internal environment. Because the sensory modality of URY is unknown in *C. elegans*, it is difficult to explain the possible purpose of this dorsal-ventral asymmetry in *A. avenae*. Also unique to *A. avenae* is the anterior accessory process that enters the sensory channel of the quadrant outer labial sensilla.

FLP. The FLP dendrites, as identified in *A. avenae*, are not ciliated and have simple termini as in *A. complexus*; this contrasts with *C. elegans*, in which FLP has a cilium. The axial position of these neurons, including their proximity to labial sensillum support cells, lends support to their homology, although positional similarity is not exact. As in *C. elegans*, their termini are associated with the lateral inner labial socket cells in *A. avenae*, but not with the HypB toroid as in *A. complexus*. The termini of these dendrites deep within the body suggest that, as in *A. complexus*, they are likely to lack the homologous mechanosensory function important in *C. elegans* (Kaplan and Horvitz, 1993). Reduction of function is supported by the absence of the terminal branching that is strongly characteristic of FLP in *C. elegans*.

Comparison with other Tylenchomorpha

Notwithstanding much previous and informative ultrastructural research on sensilla in Tylenchomorpha, detailed comparison of *A. avenae* with previously studied taxa is in many cases precluded by technical differences. Many cells and their sometimes highly elaborate components can be thin, indistinct, or otherwise hard to trace. Novel specimen preparation and computer-based reconstruction has allowed unparalleled characterization of sensory structures, including those not previously described, as well as their relationships to each other and other tissues. In the present study, a model taxon has been chosen explicitly based on its phylogenetic position; a nematode representing a basal lineage (Aphelenchoidea) of Tylenchomorpha by both molecular and morphological (Siddiqi, 1980; Maggenti, 1981) accounts is deemed optimal for polarization of characters when they are variable across other tylenchids. Where it is possible to make them, comparisons suggest the general conservation of the sensory anatomy in Tylenchomorpha. Clearly established differences between *A. avenae* and other studied Tylenchomorpha may in some cases be considered a function of their interrelationships (Fig. 8).

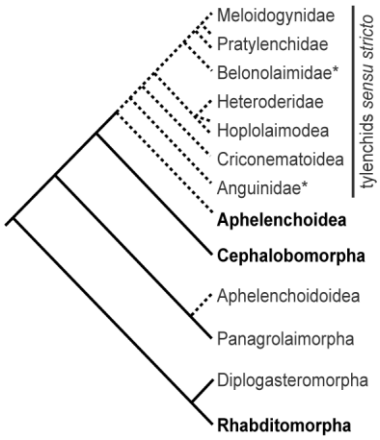

Figure 8.
Summarized phylogenetic tree of Tylenchomorpha and outgroups. Relationships among Tylenchomorpha are a summarized consensus of phylogenies from Subbotin et al. (2006) and Bert et al. (2008). Relationships between infraorders represent a consensus of phylogenies from several phylum-wide analyses (Aleshin et al., 1998; Blaxter et al., 1998; Holterman et al., 2006; Smythe et al., 2006; Meldal et al., 2007; Bert et al., 2008), although placement of the root varies between some analyses. Taxa in bold are those including models with fully reconstructed sensory anatomies; taxa on dashed branches belong to "Tylenchomorpha." Names of taxa within Tylenchomorpha are from the classifications of Hunt (1993) and Siddiqi (2000), whereas infraordinal level names (-morpha) are from De Ley and Blaxter (2002); "tylenchids sensu stricto" designates all non-aphelenchid Tylenchomorpha. Higher taxa represented by the names are simplified to not include outlying members with different phylogenetic positions. *, A taxon that is putatively paraphyletic, but whose genera discussed in the text fall into the positions indicated on the tree.

Cuticular sensilla. As in outgroups, in all Tylenchomorpha examined the inner labial sensillum contains two dendrites, with one (IL1) terminating proximally to the cuticular terminus of the other (IL2). The sensilla always lie peripheral to the guiding apparatus and are externally exposed in cuticular pores surrounding the stomatal opening. Despite the apparent high degree of conservation of this sensillum, whether some components, particularly the distinct loop of IL1 and its lateral ciliate extension, are conserved throughout Tylenchomorpha is still unknown. Further specialization of this dendrite in tylenchids might be anticipated given its recognizable divergence at least relative to outgroups.

The expression of the outer labial dendrites is variable across Tylenchomorpha, with no more than one being observed in the cephalic cuticle. In some taxa, including males of *Meloidogyne incognita* (Meloidogynidae; see Fig. 8 for phylogenetic placement of taxa) (Baldwin and Hirschmann, 1973) and second stage juveniles (Endo and Wergin, 1977) as well as *Tylenchulus semipenetrans* (Criconematoidea) (Natasasmita and De Grisse, 1978), the outer labial sensillum is apparently absent. Its presence in *Pratylenchus* (Pratylenchidae) (De Grisse, 1977; Trett and Perry, 1985), putatively comprising a monophyletic clade with *Meloidogyne* (Holterman et al., 2006; Subbotin et al., 2006), implies possible multiple losses of this feature. Baldwin and Hirschmann (1975) noted the presence of a second, internal outer labial dendrite (OL1) terminating internally within *Heterodera glycines* (Heteroderidae), lending support to the conservation of this more elusive neuron in other Tylenchomorpha. More complete sampling of the presence of OL1 throughout the group would provide a more rigid test of its apparent plasticity.

Cephalic sensilla in Tylenchomorpha, as in outgroups, always have at least one dendrite (CEP1) terminating within the cuticle to function as a mechanoreceptor. The dendrite has a swollen terminus that is filled with a characteristic osmophilic substance and extends anteriad in an arc through the outer cephalic cuticle. A second cephalic dendrite (putatively CEP2) has also been found in tylenchids sensu stricto, but always terminates deeper within the cephalic framework. In *Anguina* and *Ditylenchus* ("Anguinidae") as well as *Tylenchorhynchus* and *Macrotrophurus* ("Belonolaimidae") the second cephalic dendrite apparently extends beyond its basal body (De Grisse, 1977); in *Heterodera*, *Pratylenchus*, and various Hoplolaimidae it lacks a cilium (De Grisse, 1977; Trett and Perry, 1985); it is completely absent in Criconematoidea (De Grisse, 1977) and *Meloidogyne incognita* (Baldwin and Hirschmann, 1973). However, in *Aphelenchoides fragariae* (Aphelenchoidoidea), a second cephalic dendrite terminates in a pore in the cuticle (De Grisse et al., 1979), as in *A. avenae* and *A. complexus*. The apparent decreased reliance on this chemosensory neuron in more apical plant parasites, with respect to basal, fungal feeding taxa, may reflect a real trend in the evolution of specialization. Interestingly, this reduction contrasts with the expression of inner labial chemoreceptors, IL2, which are present throughout Tylenchomorpha. In the case of functional redundancy of these chemoreceptors, the position of the inner labial pores immediately around the stomatal opening may signify greater utility for chemoreception than other anterior receptors, especially during feeding. Characterization of IL2 and, where present, CEP2 in Tylenchomorpha would be required to test their relevant functional importance.

Internal sensory receptors. The most often noted internal receptors are the conspicuous termini of the BAG dendrites. These were explicitly described as sensory termini ("accessory axons") in *Meloidogyne* (Endo and Wergin, 1977), and found to be continuous across framework sectors in *Aphelenchoides* (De Grisse et al., 1979) and *Pratylenchus* (Trett and Perry, 1985). Although numbers of cilia with elaborately anterior branches reportedly have differed, lateral dendrites internally adjacent to the amphid bundles in *Meloidogyne* and *Pratylenchus* are likely to be homologous with BAG; this is supported by the close association of the two prominent, lateral cilia with the epidermis (presumably HypC) in the former. Quadrant dendrites observed in all cases may be URX, URY, or both, although further study will be required for thoroughly characterizing these more elusive receptors in other Tylenchomorpha.

Expanding models of experimental neurology in nematodes

Understanding homologies of the sensory system in Tylenchomorpha with respect to *C. elegans* opens the possibility for extending this well-established experimental model. Knowledge of behavior patterns in *C. elegans*, grounded in a thorough understanding of neural networks and connectivity (Ward et al., 1975; Ware et al., 1975; White et al., 1986), offers an advanced stepping-off point for experimental neurology in Tylenchomorpha. The utility of *A. avenae* in particular as a model is underscored by its ready availability and ease of maintenance in culture. Adaptations of the sensory system in

this group, which includes the most species and most specialized of plant parasitic nematodes, necessarily has implications for the evolution of parasitism. Empirically targeting individual neurons, particularly those of unknown or speculative function, may shed light on more specific aspects of plant parasitic nematode behavior at the interface with its host.

ACKNOWLEDGMENTS

The authors thank Dr. Dan Bumbarger for allowing access to the aligned, original serial section micrographs for *A. complexus* and valuable criticism of the manuscript. The authors also thank Dr. Krassimir Bozhilov and Stephen McDaniel at the UCR Center for Advanced Microscopy and Microanalysis for support in TEM and imaging.

LITERATURE CITED

Aleshin VV, Kedrova OS, Milyutina IA, Vladychenskaya, NS, Petrov, NB. 1998. Relationships among nematodes based on the analysis of 18S rRNA gene sequences: molecular evidence for monophyly of chromadorian and secernentean nematodes. Russ J Nematol 6:175–184.

Aronoff R, Mellem, JE, Maricq AV, Sprengel R, Seeburg PH. 2004. Neuronal toxicity in *Caenorhabditis elegans* from an editing site mutant in glutamate receptor channels. J Neurosci 24:8135–8140.

Ashton FT, Bhopale VM, Fine AE, Schad GA. 1995. Sensory neuroanatomy of a skin-penetrating nematode parasite: *Strongyloides stercoralis*. I. Amphidial neurons. J Comp Neurol 357:281–295.

Baldwin JG, Hirschmann H. 1973. Fine structure of cephalic sense organs in *Meloidogyne incognita* males. J Nematol 5:285–302.

Baldwin JG, Hirschmann H. 1975. Fine structure of cephalic sense organs in *Heterodera glycines* males. J Nematol 7:40–53.

Baldwin JG, Hirschmann H. 1976. Comparative fine structure of the stomatal region of males of *Meloidogyne incognita* and *Heterodera glycines*. J Nematol 8:1–17.

Baldwin JG, Nadler SA, Adams BJ. 2004a. Evolution of plant parasitism among nematodes. Annu Rev Phytopathol 16:83–105.

Baldwin JG, Ragsdale EJ, Bumbarger, D. 2004b. Revised hypotheses for phylogenetic homology of the stomatostylet in tylenchid nematodes. Nematology 6:623–632.

Bert W, Leliaert F, Vierstraete AR, Vanfleteren JR, Borgonie G. 2008. Molecular phylogeny of the Tylenchina and evolution of the female gonoduct (Nematoda: Rhabditida). Mol Phylogenet Evol 48:728–744.

Blaxter M, De Ley, P, Garey JR, Liu LX, Scheldeman P, Vierstraete A, Vanfleteren JR, Mackey LY, Dorris M, Frisse LM, Vida JT, Thomas WK. 1998. A molecular evolutionary framework for the phylum Nematoda. Nature 392:71–75.

Bumbarger DJ, Crum J, Ellisman MH, Baldwin JG. 2006. Three-dimensional reconstruction of the nose epidermal cells in the microbial feeding nematode, *Acrobeles complexus* (Nematoda: Rhabditida). J Morphol 267:1257–1272.

Bumbarger DJ, Crum J, Ellisman MH, Baldwin JG. 2007. Three-dimensional fine structural reconstruction of the nose sensory structures of *Acrobeles complexus* compared to *Caenorhabditis elegans* (Nematoda: Rhabditida). J Morphol 268:649–663.

Bumbarger DJ, Wijeratne S, Carter C, Crum J, Ellisman MH, Baldwin JG. 2009. Three-dimensional reconstruction of the amphid sensilla in the microbial feeding nematode, *Acrobeles complexus* (Nematoda: Rhabditida). J Comp Neurol 512:271–281.

Chalfie M, Thomson JN. 1982. Structural and functional diversity in the neuronal microtubules of *Caenorhabditis elegans*. J Cell Biol 93:15–23.

Chang AJ, Chronis N, Karow DS, Marletta MA, Bargmann CI. 2006. A distributed chemosensory circuit for oxygen preference in *C. elegans*. PLoS Biol 4:e274.

Cheung BH, Cohen M, Rogers C, Albayram O, de Bono M. 2005. Experience-dependent modulation of *C. elegans* behavior by ambient oxygen. Curr Biol 15:905–917.

Coates JC, de Bono M. 2002. Antagonistic pathways in neurons exposed to body fluid regulate social feeding in *Caenorhabditis elegans.* Nature 419:925–929.

de Bono M, Tobin DM, Davis MW, Avery L, Bargmann CI. 2002. Social feeding in *Caenorhabditis elegans* is induced by neurons that detect aversive stimuli. Nature 419:899–903.

De Grisse AT. 1975. The ultrastructure of some ciliary receptors in the cephalic region of tylenchids (Nematoda). Meded Fac Landbouww Rijksuniv Gent 40:473–487.

De Grisse AT. 1977. De ultrastruktuur van het zenuwstelsel in de kop van 22 soorten plantenparasitaire nematoden, behorende tot 19 genera (Nematoda: Tylenchina). D.Sc. Thesis, Rijksuniversiteit Gent, 420 pp.

De Grisse A, Natasasmita S, B'Chir M. 1979. L'ultrastructure des nerfs de la région céphalique chez *Aphelenchoides fragariae* (Nematoda: Tylenchida). Rev Nematol 2:123–141.

De Ley P, Blaxter ML. 2002. Systematic position and phylogeny. In: Lee DL, editor. The biology of nematodes. London: Taylor & Francis. p 1–30.

Dickinson S. 1959. The behavior of the larvae of *Heterodera schachtii* on nitrocellulose membranes. Nematologica 4:60–66.

Endo BY. 1980. Ultrastructure of the anterior neurosensory organs of the larvae of the soybean cyst nematode, *Heterodera glycines*. J Ultrastruct Res 72:349–366.

Endo BY, Wergin WP. 1977. Ultrastructure of anterior sensory organs of the root-knot nematode, *Meloidogyne incognita*. J Ultrastruct Res 59:231–249.

Fisher JM, Evans AA. 1967. Penetration and feeding by *Aphelenchus avenae*. Nematologica 13:425–428.

Giammara BL, Hanker JS. 1986. Epoxy-slide embedment of cytochemically stained tissues and cultured cells for light and electron microscopy. Stain Technol 61:51–58.

Gray JM, Karow DS, Lu H, Chang AJ, Chang JS, Ellis RE, Marletta MA, Bargmann CI. 2004. Oxygen sensation and social feeding mediated by a *C. elegans* guanylate cyclase homologue. Nature 430:317–322.

Hall DH, Russell RL. 1991. The posterior nervous system of the nematode *Caenorhabditis elegans*: serial reconstruction of identified neurons and complete pattern of synaptic interactions. J Neurosci 11:1–22.

Hart AC, Sims S, Kaplan JM. 1995. Synaptic code for sensory modalities revealed by *C. elegans* GLR-1 glutamate receptor. Nature 378:82–85.

Holterman M, van der Wurff A, van den Elsen S, van Megen H, Bongers T, Holovachov O, Bakker J, Helder J. 2006. Phylum-wide analysis of SSU rDNA reveals deep phylogenetic relationships among nematodes and accelerated evolution toward crown clades. Mol Biol Evol 23:1792–1800.

Hunt DJ. 1993. Aphelenchida, Longidoridae, and Trichodoridae: their systematics and bionomics. Wallingford, UK: CAB International.

Kaplan JM, Horvitz HR. 1993. A dual mechanosensory and chemosensory neuron in *Caenorhabditis elegans*. Proc Natl Acad Sci U S A 90:2227–2231.

Kremer JR, Mastronarde DN, McIntosh JR. 1996. Computer visualization of three-dimensional image data using IMOD. J Struct Biol 116:71–76.

Maggenti A. 1981. General nematology. New York: Springer-Verlag.

Meldal BH, Debenham NJ, De Ley P, De Ley IT, Vanfleteren JR, Vierstraete AR, Bert W, Borgonie G, Moens T, Tyler PA, Austen MC, Blaxter ML, Rogers AD, Lambshead PJ. 2007. An improved molecular phylogeny of the Nematoda with special emphasis on marine taxa. Mol Phylogenet Evol 42:622–636.

Nadler SA, De Ley P, Mundo-Ocampo M, Smythe AB, Stock SP, Bumbarger D, Adams BJ, De Ley IT, Holovachov O, Baldwin, JG. 2006. Phylogeny of Cephalobina (Nematoda): molecular evidence for recurrent evolution of probolae and incongruence with traditional classifications. Mol Phylogenet Evol 40:696–711.

Natasasmita S, De Grisse A. 1978. The supplementary nerves in the head region of *Tylenchulus semipenetrans* (Nematoda: Tylenchulidae). Meded Fac Landbouww Rijksuniv Gent 43:769–777.

Perkins LA, Hedgecock EM, Thomson JN, Culotti JG. 1986. Mutant sensory cilia in the nematode *Caenorhabditis elegans*. Dev Biol 117:456–487.

Ragsdale EJ, Crum J, Ellisman, MH, Baldwin JG. 2008. Three-dimensional reconstruction of the stomatostylet and anterior epidermis in the nematode *Aphelenchus avenae* (Nematoda: Aphelenchidae) with implications for the evolution of plant parasitism. J Morphol 269:1181–1196.

Rogers C, Persson A, Cheung B, de Bono M. 2006. Behavioral motifs and neural pathways coordinating O2 responses and aggregation in *C. elegans*. Curr Biol 16:649–659.

Sawin ER, Ranganathan R, Horvitz HR. 2000. *C. elegans* locomotory rate is modulated by the environment through a dopaminergic pathway and by experience through a serotonergic pathway. Neuron 26:619–631.

Siddiqi MR. 1980. The origin and phylogeny of the nematode orders Tylenchida Thorne, 1949 and Aphelenchida n. ord. Helminthol Abstr Ser B, Plant Nematol 49:143–170.

Siddiqi, MR. 2000. Tylenchida: parasites of plants and insects. Wallingford, UK: CAB International.

Smythe AB, Sanderson MJ, Nadler SA. 2006. Nematode small subunit phylogeny correlates with alignment parameters. Syst Biol 55:972–992.

Strote G, Bonow I. 1993. Ultrastructural observations on the nervous system and the sensory organs of the infective stage (L3) of *Onchocerca volvulus* (Nematoda: Filarioidea). Parasitol Res 79:213–220.

Subbotin SA, Sturhan D, Chizhov VN, Vovlas N, Baldwin, JG. 2006. Phylogenetic analysis of Tylenchida Thorne, 1949 as inferred from D2 and D3 expansion fragments of the 28S rRNA gene sequences. Nematology 8:455–474.

Trett MW, Perry RN. 1985. Functional and evolutionary implications of the anterior sensory anatomy of species of the root-lesion nematode (genus *Pratylenchus*). Rev Nematol 8:341–355.

Ward S, Thomson N, White JG, Brenner S. 1975. Electron microscopical reconstruction of the anterior sensory anatomy of the nematode *Caenorhabditis elegans*. J Comp Neurol 160:313–337.

Ware RW, Clark D, Crossland K, Russell RL. 1975. The nerve ring of the nematode *Caenorhabditis elegans*: sensory input and motor output. J Comp Neurol 162:71–110.

White JG, Southgate E, Thomson JN, Brenner S. 1986. The structure of the nervous system of *Caenorhabditis elegans*. Philos Trans Royal Soc Lond B 341:1–340.

Wright KA. 1975. Cephalic sense organs of the rat hookworm, *Nippostronglyus brasiliensis*—form and function. Canad J Zool 53:1131–1146.